# We are IntechOpen,
the world's leading publisher of
Open Access books
Built by scientists, for scientists

## 6,900
Open access books available

## 186,000
International authors and editors

## 200M
Downloads

Our authors are among the

## 154
Countries delivered to

## TOP 1%
most cited scientists

## 12.2%
Contributors from top 500 universities

**BOOK CITATION INDEX**
CLARIVATE ANALYTICS
INDEXED

**WEB OF SCIENCE**™

Selection of our books indexed in the Book Citation Index
in Web of Science™ Core Collection (BKCI)

## Interested in publishing with us?
Contact book.department@intechopen.com

# Flavor Physics and Charged Particle

*Takaaki Nomura*

## Abstract

We have new charged particles in many scenarios of physics beyond the Standard Model where these particles are sometimes motivated to explain experimental anomalies. Furthermore, such new charged particles are important target at the collider experiments such as the Large Hadron Collider in searching for a signature of new physics. If these new particles interact with known particles in the Standard Model, they would induce interesting phenomenology of flavor physics in both lepton and quark sectors. Then, we review some candidate of new charged particles and its applications to flavor physics. In particular, vector-like lepton and leptoquarks are discussed for lepton flavor physics and $B$-meson physics.

**Keywords:** flavor physics, charged particle from beyond the standard model, $B$-meson decay, vector-like lepton/quark, leptoquarks, charged scalar boson

## 1. Introduction

Charged particles are often considered in the physics beyond the Standard Model (BSM) of particle physics as new heavy particles which are not observed at the experiments. Such charged particles can have rich phenomenology since it would interact with particles in the Standard Model (SM). Furthermore they are motivated to explain some experimental anomalies indicating deviation from predictions in the SM. For example, some charged particle interaction can accommodate with the anomalous magnetic moment of the muon, $(g-2)_\mu$, which shows a long-standing discrepancy between experimental observations [1, 2] and theoretical predictions [3–6],

$$\Delta a_\mu \equiv \Delta a_\mu^{\text{exp}} - \Delta a_\mu^{\text{th}} = (28.8 \pm 8.0) \times 10^{-10}, \tag{1}$$

where $a_\mu = (g-2)_\mu/2$. This difference reaches to $3.6\sigma$ deviation from the prediction. In addition, new charged particles are introduced when we try to explain anomalies in $B$-meson decay like $B \to K^{(*)}\mu^+\mu^-$ and $B \to D^{(*)}\tau\nu$ [7–16].

In this chapter, we review some candidates of new charged particles from BSM physics. After listing some examples of them, the applications to some flavor physics will be discussed focusing on some specific cases. We find it interesting to consider new charged particles which are related to flavor physics in both lepton and quark sectors.

## 2. Some charged particles from beyond the standard model physics

In this section we review some examples of charged particles which are induced from BSM physics.

### 2.1 Charged scalar bosons

Singly charged scalar appears from two-Higgs doublet model (2HDM) [17, 18] in which two $SU(2)_L$ doublet Higgs fields are introduced:

$$H_1 = \begin{pmatrix} H_1^+ \\ (v_1 + \phi_1 + i\eta_1)/\sqrt{2} \end{pmatrix}, \quad H_2 = \begin{pmatrix} H_2^+ \\ (v_2 + \phi_2 + i\eta_2)/\sqrt{2} \end{pmatrix}, \tag{2}$$

where $v_{1,2}$ is the vacuum expectation values (VEVs) of Higgs fields. In general, one can write Yukawa interaction in terms of Higgs doublet fields as

$$-\mathcal{L}_Y = \overline{Q}_L Y_1^d D_R H_1 + \overline{Q}_L Y_2^d D_R H_2 + \overline{Q}_L Y_1^u U_R \tilde{H}_1 + \overline{Q}_L Y_2^u U_R \tilde{H}_2$$
$$+ \overline{L} Y_1^\ell \ell_R H_1 + \overline{L} Y_2^\ell \ell_R H_2 + H.c., \tag{3}$$

where all flavor indices are hidden, $P_{R(L)} = (1 \pm \gamma_5)/2$; $Q_L^i = \left(u_L^i, d_L^i\right)$ and $L_L = \left(\nu_L^i, e_L^i\right)$ are the $SU(2)_L$ quark and lepton doublets with flavor index $i$, respectively; $f_R$ ($f = U, D, \ell$) denotes the $SU(2)_L$ singlet fermion; $Y_{1,2}^f$ are the $3 \times 3$ Yukawa matrices; and $\tilde{H}_i = i\tau_2 H_i^*$ with $\tau_2$ being the Pauli matrix. There are two CP-even scalars, one CP-odd pseudoscalar, and two charged Higgs particles in the 2HDM, and the relations between physical and weak eigenstates can be given by

$$h = -s_\alpha \phi_1 + c_\alpha \phi_2,$$
$$H = c_\alpha \phi_1 + s_\alpha \phi_2, \tag{4}$$
$$H^\pm(A) = -s_\beta \phi_1^\pm(\eta_1) + c_\beta \phi_2^\pm(\eta_2),$$

where $\phi_i(\eta_i)$ and $\eta_i^\pm$ denote the real (imaginary) parts of the neutral and charged components of $H_i$, respectively; $c_\alpha(s_\alpha) = \cos\alpha(\sin\alpha)$, $c_\beta = \cos\beta = v_1/v$, $s_\beta = \sin\beta = v_2/v$, and $v_i$ are the vacuum expectation values (VEVs) of $H_i$ and $v = \sqrt{v_1^2 + v_2^2} \approx 246$ GeV. In our notation, $h$ is the SM-like Higgs, while $H$, $A$, and $H^\pm$ are new particles which appear in the 2HDM. In particular, Yukawa interactions with charged Higgs are given by

$$-\mathcal{L}_Y^{H^\pm} = \sqrt{2}\,\overline{d}_L V^\dagger \left[ -\frac{1}{vt_\beta} \mathbf{m_u} + \frac{\mathbf{X}^u}{s_\beta} \right] u_R H^-$$

$$+ \sqrt{2}\,\overline{u}_L V \left[ -\frac{t_\beta}{v} \mathbf{m_d} + \frac{\mathbf{X}^d}{c_\beta} \right] d_R H^+ \tag{5}$$

$$+ \sqrt{2}\,\overline{\nu}_L \left[ -\frac{t_\beta}{v} \mathbf{m_\ell} + \frac{\mathbf{X}^\ell}{c_\beta} \right] \ell_R H^+ + H.c.,$$

where $V$ is the CKM matrix and the matrix $\mathbf{X}^f$ is defined by original Yukawa coupling and unitary matrix diagonalizing fermion mass

$$\mathbf{X}^u = V_L^u \frac{Y_1^u}{\sqrt{2}} V_R^{u\dagger}, \quad \mathbf{X}^d = V_L^d \frac{Y_2^d}{\sqrt{2}} V_R^{d\dagger}, \quad \mathbf{X}^\ell = V_L^\ell \frac{Y_2^\ell}{\sqrt{2}} V_R^{\ell\dagger}. \tag{6}$$

A doubly charged scalar boson also appears from $SU(2)_L$ triplet scalar field:

$$\Delta = \begin{pmatrix} \delta^+/\sqrt{2} & \delta^{++} \\ (v_\Delta + \delta^0 + i\eta^0)/\sqrt{2} & -\delta^+/\sqrt{2} \end{pmatrix}, \tag{7}$$

where $v_\Delta$ is the VEV of the triplet scalar. Such a triplet scalar is motivated to generate neutrino mass known as Higgs triplet model or type-II seesaw mechanism [19–26]. We can write Yukawa interaction of triplet scalar and lepton doublets by

$$L_Y = h_{ij} L_{L_i}^T C i\sigma_2 \Delta L_{L_j} + h.c. \;, \tag{8}$$

where $L_{L_i} = (\nu_i, \ell_i)_L^T$ with flavor index $i$ and $C = i\gamma^2\gamma^0$ is the Dirac charge conjugation operator. In terms of the components, the Yukawa interaction can be expanded as

$$\begin{aligned}
L_Y = & h_{ij}\left( -\frac{1}{\sqrt{2}}\ell_{iL}^T C\delta^+ \nu_{jL} - \ell_{iL}^T C\delta^{++}\ell_{jL} + \nu_{iL}^T C\delta^0 \nu_{jL} - \frac{1}{\sqrt{2}}\nu_{iL}^T C\delta^+ \ell_{jL} \right) \\
& + h_{ji}^*\left( \frac{1}{\sqrt{2}}\nu_{iL}^\dagger C\delta^- \ell_{jL}^* + \ell_{iL}^\dagger C\delta^{--}\ell_{jL}^* - \nu_{iL}^\dagger C\delta^0 \nu_{jL}^* + \frac{1}{\sqrt{2}}\ell_{iL}^\dagger C\delta^- \nu_{jL}^* \right)
\end{aligned} \tag{9}$$

where $C^\dagger = -C$ is used. Another example of model including doubly charged scalar is Zee-Babu type model [27, 28] for neutrino mass generation at two-loop level. In such a type of model, one introduces singly and doubly charged scalars $(h^\pm, k^{\pm\pm})$ which are $SU(2)_L$ singlet. The Yukawa couplings associated with charged scalar fields are given by

$$L_Y = f_{ij}\overline{L}_{L_i}^c (i\sigma_2) L_{L_j} h^+ + g_{ee}\bar{e}_R^c e_R k^{++} + g_{ij}\bar{e}_{R_i}^c e_{R_j} k^{++} + h.c., \tag{10}$$

where $f_{ij}$ is antisymmetric under flavor indices. These Yukawa interactions can be used to generate neutrino mass with the nontrivial interaction in scalar potential:

$$V \supset \mu k^{++} h^- h^- + c.c.. \tag{11}$$

Note that these charged scalars also contribute to lepton flavor violation processes.

## 2.2 Vector-like leptons

The vector-like leptons (VLLs) are discussed in Ref. [29]. They are new charged particles without conflict of gauge anomaly problem and induce rich lepton flavor physics. To obtain mixing with the SM leptons, the representations of VLL under $SU(2)_L \times U(1)_Y$ gauge symmetry can be singlet, doublet, and triplet under $SU(2)_L$. In order to avoid the stringent constraints from rare $Z \to \ell_i^\pm \ell_j^\mp$ decays, we here consider the triplet representations $(1, 3, -1)$ and $(1, 3, 0)$ with hypercharges $Y = -1$ and $Y = 0$, respectively. The new Yukawa couplings thus can be written such that

$$-\mathcal{L}_Y = \overline{L}\mathbf{Y}_1\Psi_{1R}H + \overline{L}\mathbf{Y}_2\Psi_{2R}\tilde{H} + m_{\Psi_1}Tr\overline{\Psi}_{1L}\Psi_{1R} + m_{\Psi_2}Tr\overline{\Psi}_{2L}\Psi_{2R} + H.c., \tag{12}$$

where we have suppressed the flavor indices; $H$ is the SM Higgs doublet field, $\tilde{H} = i\tau_2 H^*$ and the neutral component of Higgs field is $H^0 = (v+h)/\sqrt{2}$. The representations of two VLLs are

$$\Psi_1 = \begin{pmatrix} \Psi_1^- / \sqrt{2} & \Psi_1^0 \\ \Psi_1^{--} & -\Psi_1^- / \sqrt{2} \end{pmatrix}, \quad \Psi_2 = \frac{1}{\sqrt{2}} \begin{pmatrix} \Psi_2^0 / \sqrt{2} & \Psi_2^+ \\ \Psi_2^- & -\Psi_2^0 / \sqrt{2} \end{pmatrix}, \tag{13}$$

with $\Psi_2^+ = C\overline{\Psi}_2^-$ and $\Psi_2^0 = C\overline{\Psi}_2^0$. Since $\Psi_2$ is a real representation of $SU(2)_L$, the factor of $1/\sqrt{2}$ in $\Psi_2$ is required to obtain the correct mass term for Majorana fermion $\Psi_2^0$. Due to the new Yukawa terms of $\mathbf{Y}_{1,2}$, the heavy neutral and charged leptons can mix with the SM leptons, after electroweak symmetry breaking (EWSB). Then the lepton mass matrices become $5 \times 5$ matrices and are expressed by

$$M_\ell = \begin{pmatrix} \mathbf{m}_\ell & \mathbf{Y}^\ell v \\ 0 & \mathbf{m}_\Psi \end{pmatrix}, \quad M_\nu = \begin{pmatrix} \mathbf{m}_\nu & \mathbf{Y}^\nu v \\ 0 & \mathbf{m}_\Psi \end{pmatrix}, \tag{14}$$

where the basis is chosen such that the SM lepton mass matrices are in diagonalized form, $\mathbf{m}_\ell$ is the SM charged lepton mass matrix, $\mathbf{m}_\Psi = \mathrm{diag}(m_{\Psi_1}, m_{\Psi_2})$, and

$$\mathbf{Y}^\ell = \frac{1}{2} \begin{pmatrix} -Y_{11} & Y_{21} \\ -Y_{12} & Y_{22} \\ -Y_{13} & Y_{23} \end{pmatrix}, \quad \mathbf{Y}^\nu = \sqrt{2} \begin{pmatrix} Y_{11} & Y_{21}/2 \\ Y_{12} & Y_{22}/2 \\ Y_{13} & Y_{23}/2 \end{pmatrix}. \tag{15}$$

Note that the elements of $\mathbf{Y}^\chi$ should be read as $Y_{ij} = (\mathbf{Y}_i)_j$, where the index $i = 1, 2$ distinguishes the Yukawa couplings of the different VLLs and the index $j = 1, 2, 3$ stands for the flavors of the SM leptons.

To diagonalize $M_\ell$ and $M_\nu$, the unitary matrices $V_{R,L}^\chi$ with $\chi = \ell, \nu$ so that $M_\chi^{\mathrm{dia}} = V_L^\chi M_\chi V_R^{\chi\dagger}$ are introduced. The information of $V_L^\chi$ and $V_R^\chi$ can be obtained from $M_\chi M_\chi^\dagger$ and $M_\chi^\dagger M_\chi$, respectively. According to Eq. (14), it can be found that the flavor mixings between heavy and light leptons in $V_R^\chi$ are proportional to the lepton masses. Since the neutrino masses are tiny, it is a good approximation to assume $V_R^\nu \approx 1$. If one further sets $m_e = m_\mu = 0$ in our phenomenological analysis, only $\tau$-related processes have significant contributions among them. Unlike $V_R^\chi$, the off-diagonal elements in flavor-mixing matrices $V_L^\chi$ are associated with $\mathbf{Y}_{1,2} v / \mathbf{m}_\Psi$. In principle, the mixing effects can be of the order of 0.1 without conflict. In our example later, we examine these effects on $h \to \tau\mu$. To be more specific, we choose parametrization that the unitary matrices in terms of $\mathbf{Y}_{1,2}$ as

$$V_L^\chi \approx \begin{pmatrix} 1_{3\times3} - \varepsilon_L^\chi \varepsilon_L^{\chi\dagger}/2 & -\varepsilon_L^\chi \\ \varepsilon_L^{\chi\dagger} & 1_{3\times3} - \varepsilon_L^{\chi\dagger} \varepsilon_L^\chi/2 \end{pmatrix}, \quad V_R^\ell \approx \begin{pmatrix} 1_{3\times3} & -\varepsilon_R^\ell \\ \varepsilon_R^{\ell\dagger} & 1_{3\times3} \end{pmatrix}, \tag{16}$$

where $V_R^\nu \approx 1$ is used in our approximation, $\varepsilon_L^\chi \approx v\mathbf{Y}^\chi/\mathbf{m}_\Psi$, and $\varepsilon_R^\ell \approx v\mathbf{m}_\ell^\dagger \mathbf{Y}^\ell/\mathbf{m}_\Psi^2$. Combining the SM Higgs couplings and new Yukawa couplings of Eq. (12), the Higgs couplings to all singly charged leptons are obtained such as

$$-\mathcal{L}_{h\ell'\ell'} = h\overline{\ell}_L' V_L^\ell \begin{pmatrix} \mathbf{m}_\ell/v & \mathbf{Y}^\ell \\ 0 & 0 \end{pmatrix} V_R^{\ell\dagger} \ell_R' + H.c., \tag{17}$$

where $\ell'^T = (e, \mu, \tau, \tau', \tau'')$ is the state of a physical charged lepton in lepton flavor space. We use the notations of $\tau'$ and $\tau''$ to denote the heavy-charged VLLs in mass basis. Using the parametrization of Eq. (16), the Higgs couplings to the SM-charged leptons can be formulated by

$$-\mathcal{L}_{h\ell\ell} = C_{ij}^h \overline{\ell}_{iL} \ell_{jR} h + H.c.,$$

$$C_{ij}^h = \frac{m_{\ell j}}{v} \left[ \delta_{ij} - \frac{3}{8} \left( \frac{v^2 Y_{1i} Y_{1j}}{m_{\Psi_1}^2} + \frac{v^2 Y_{2i} Y_{2j}}{m_{\Psi_2}^2} \right) \right]. \tag{18}$$

If one sets $m_e = m_\mu = 0$, it is clear that in addition to the coupling $h\tau\tau$ being modified, the tree-level flavor-changing couplings $h$- $\tau$- $\mu$ and $h$- $\tau$- $e$ are also induced, and the couplings are proportional to $m_\tau / v \approx 7.2 \times 10^{-3}$. In order to study the VLL contributions to $h \to \gamma\gamma$, the couplings for $h\tau'\tau'$ and $h\tau''\tau''$ are expressed as

$$-\mathcal{L}_{h\Psi\Psi} = \frac{v \sum_i Y_{1i}^2}{2 m_{\Psi_1}} h\tau'\tau' + \frac{v \sum_i Y_{2i}^2}{2 m_{\Psi_2}} h\tau''\tau''. \tag{19}$$

### 2.3 Vector-like quarks

Here we consider vector-like triplet quarks (VLTQs) that are discussed in Ref. [30] The gauge invariant Yukawa couplings of VLTQs to the SM quarks, to the SM Higgs doublet and to the new Higgs singlet field are written as

$$-\mathcal{L}_{VLTQ}^Y = \overline{Q}_L \mathbf{Y}_1 F_{1R} \tilde{H} + \overline{Q}_L \mathbf{Y}_2 F_{2R} H + \tilde{y}_1 Tr(\overline{F}_{1L} F_{1R}) S + \tilde{y}_2 Tr(\overline{F}_{2L} F_{2R}) S$$
$$+ M_{F_1} Tr(\overline{F}_{1L} F_{1R}) + M_{F_2} Tr(\overline{F}_{2L} F_{2R}) + h.c., \tag{20}$$

where $Q_L$ is the left-handed SM quark doublet and it could be regarded as mass eigenstate before VLTQs are introduced; here all flavor indices are hidden, $\tilde{H} = i\tau_2 H^*$, and $F_{1(2)}$ is the $2 \times 2$ VLTQ with hypercharge $2/3(-1/3)$. The representations of $F_{1,2}$ in $SU(2)_L$ are expressed in terms of their components as follows:

$$F_1 = \begin{pmatrix} U_1/\sqrt{2} & X \\ D_1 & -U_1/\sqrt{2} \end{pmatrix}, \quad F_2 = \begin{pmatrix} D_2/\sqrt{2} & U_2 \\ Y & -D_2/\sqrt{2} \end{pmatrix}. \tag{21}$$

The electric charges of $U_{1,2}$, $D_{1,2}$, $X$, and $Y$ are found to be $2/3$, $-1/3$, $5/3$, and $-4/3$, respectively. Therefore, $U_{1,2}(D_{1,2})$ could mix with up (down) type SM quarks. Here $M_{F_{1(2)}}$ is the mass of VLTQ, and due to the gauge symmetry, the VLTQs in the same multiplet state are degenerate. By the Yukawa couplings of Eq. (20), the $5 \times 5$ mass matrices for up and down type quarks are found by

$$M_u = \begin{pmatrix} (\mathbf{m}_u^{dia})_{3\times 3} & | & v\mathbf{Y}_1/2 & v\mathbf{Y}_2/\sqrt{2} \\ ----- & | & ---- & ---- \\ 0_{2\times 3} & | & & (\mathbf{m}_F)_{2\times 2} \end{pmatrix},$$

$$M_d = \begin{pmatrix} (\mathbf{m}_d^{dia})_{3\times 3} & | & v\mathbf{Y}_1/\sqrt{2} & -v\mathbf{Y}_2/2 \\ ----- & | & ---- & ---- \\ 0_{2\times 3} & | & & (\mathbf{m}_F)_{2\times 2} \end{pmatrix}, \tag{22}$$

where $\left(\mathbf{m}_u^{\mathrm{dia}}\right)_{3\times3}$ and $\left(\mathbf{m}_d^{\mathrm{dia}}\right)_{3\times3}$ denote the diagonal mass matrices of SM quarks and $\mathrm{dia}(m_F)_{2\times2} = (m_{F_1}, m_{F_2})$. Notice that a non-vanished $v_s$ could shift the masses of VLTQs. Since $v_s \ll v$, we neglect the small effects hereafter. Due to the presence of $\mathbf{Y}_{1,2}$, the SM quarks, $U_{1,2}$, and $D_{1,2}$ are not physical states; thus one has to diagonalize $M_u$ and $M_d$ to get the mass eigenstates in general. If $vY_{1,2}^i \ll m_{F_{1,2}}$, we expect that the off-diagonal elements of unitary matrices for diagonalizing the mass matrices should be of order of $vY_{1,2}^i/m_{F_{1,2}}$. By adjusting $Y_{1,2}^i$, the off-diagonal effects could be enhanced and lead to interesting phenomena in collider physics.

## 2.4 Scalar leptoquarks

In this subsection we consider leptoquarks (LQs) which are discussed for example in Refs. [31, 32]. The three LQs are $\Phi_{7/6} = (2, 7/6)$, $\Delta_{1/3} = (3, 1/3)$, and $S^{1/3} = (1, 1/3)$ under $\left(SU(2)_L, U(1)_Y\right)$ SM gauge symmetry, where the doublet and triplet representations can be taken as

$$\Phi_{7/6} = \begin{pmatrix} \phi^{5/3} \\ \phi^{2/3} \end{pmatrix}, \quad \Delta_{1/3} = \begin{pmatrix} \delta^{1/3}/\sqrt{2} & \delta^{4/3} \\ \delta^{-2/3} & -\delta^{1/3}/\sqrt{2} \end{pmatrix}, \tag{23}$$

where the superscripts are the electric charges of the particles. Accordingly, the LQ Yukawa couplings to the SM fermions are expressed as

$$-L_{LQ} = \left[\overline{u}\,\mathbf{Vk}P_R\ell\phi^{5/3} + \overline{d}\,\mathbf{k}P_R\ell\phi^{2/3}\right] + \left[-\overline{\ell}\,\tilde{\mathbf{k}}P_Ru\phi^{-5/3} + \overline{\nu}\,\tilde{\mathbf{k}}P_Ru\phi^{-2/3}\right]$$
$$+ \left[\overline{u^c}\,\mathbf{V}^*\mathbf{y}P_L\nu\delta^{-2/3} - \frac{1}{\sqrt{2}}\overline{u^c}\,\mathbf{V}^*\mathbf{y}P_L\ell\delta^{1/3} - \frac{1}{\sqrt{2}}\overline{d^c}\,\mathbf{y}P_L\nu\delta^{1/3} - \overline{d^c}\,\mathbf{y}P_L\ell\delta^{4/3}\right],$$
$$+ \left(\overline{u^c}\,\mathbf{V}^*\tilde{\mathbf{y}}P_L\ell - \overline{d^c}\,\tilde{\mathbf{y}}P_L\nu + \overline{u^c}\,\mathbf{w}P_R\ell\right)S^{1/3} + h.c., \tag{24}$$

where the flavor indices are hidden, $\mathbf{V} \equiv U_L^u U_L^{d\dagger}$ denotes the Cabibbo-Kobayashi-Maskawa (CKM) matrix, $U_L^{u,d}$ are the unitary matrices used to diagonalize the quark mass matrices, and $U_L^d$ and $U_R^u$ have been absorbed into $\mathbf{k}$, $\tilde{\mathbf{k}}$, $\mathbf{y}$, $\tilde{\mathbf{y}}$, and $\mathbf{w}$. In this setup, we treat the neutrinos as massless particles and their flavor mixing effects are rotated away as an approximation. There is no evidence for any new CP violation, so in the following, we treat the Yukawa couplings as real numbers for simplicity.

The scalar LQs can also couple to the SM Higgs field via the scalar potential, and the cross section for the Higgs to diphoton can be modified in principle. However,

| Particle type | $(SU(3), SU(2), U(1)_Y)$ | Examples of application |
|---|---|---|
| Charged scalar | $(1, 3, 1)$, $(1, 2, 1/2)$ | Neutrino mass, lepton flavor violation |
| Vector-like lepton | $(1, 3, -1)$, $(1, 3, 0)$ | Lepton flavor violation |
| Vector-like quark | $(3, 3, 2/3)$, $(3, 3, -1/3)$ | Quark flavor physics |
| Scalar leptoquark | $(3, 2, 7/6)$, $(3, 3, 1/3)$, $(3, 1, 1/3)$ | Meson decay, lepton flavor violation |

**Table 1.**
*List of examples of charged particles from new physics discussed in this review showing $SU(3) \times SU(2) \times U(1)_Y$ representations and applications to phenomenology.*

the couplings of the LQs to the Higgs are independent parameters and irrelevant to the flavors, so by taking proper values for the parameters, the signal strength parameter for the Higgs to diphoton can fit the LHC data. For detailed analysis see **Table 1** in Ref. [31].

## 3. Examples of applying charged particles to flavor physics

In this section, we review applications of charged particles to flavor physics by considering VLLs and LQs as examples.

### 3.1 Flavor physics from vector-like lepton

Introduction of VLLs contributes to lepton flavor physics via Yukawa interactions discussed in previous section. Here we review the leptonic decay of the SM Higgs and LFV decay of charged lepton as an illustration based on Ref. [29].

*3.1.1 Modification to $h \to \tau^+\tau^-$ branching ratio*

From Eq. (18), it can be seen that the modified Higgs couplings to the SM leptons are proportional lepton masses. By comparison with other lepton channels, it can be seen that the $\tau\tau$ mode is the most significant one, and thus we estimate the influence on $h \to \tau^+\tau^-$. Using the values that satisfy $BR(h \to \mu\tau) \approx 10^{-4}$, the deviation of $\Gamma(h \to \tau^+\tau^-)$ from the SM prediction can be obtained as

$$\kappa_{\tau\tau} \equiv \frac{\Gamma(h \to \tau^+\tau^-)}{\Gamma^{SM}(h \to \tau^+\tau^-)} = \left|1 - \frac{6v^2 Y_3^2}{8m_\Psi^2}\right|^2 \approx 0.88. \tag{25}$$

If the SM Higgs production cross section is not changed, the signal strength for $pp \to h \to \tau^+\tau^-$ in our estimation is $\mu_{\tau\tau} \approx 0.88$, where the measurements from ATLAS and CMS are $1.44^{+0.42}_{-0.37}$ [33] and $0.91 \pm 0.27$ [34], respectively. Although the current data errors for the $\tau\tau$ channel are still large, the precision measurement of $\mu_{\tau\tau}$ can test the effect or give strict limits on the parameters.

*3.1.2 $\tau \to \mu\gamma$ process in vector-like lepton model*

In the following, we investigate the contributions of new couplings in Eq. (18) to the rare tau decays and to the flavor-conserving muon anomalous magnetic moment. We first investigate the muon $g - 2$, denoted by $\Delta a_\mu$. The lepton flavor-changing coupling $h\mu\tau$ can provide contribution to $\Delta a_\mu$ through the Higgs-mediated loop diagrams. However, as shown in Eq. (18), the induced couplings are associated with $m_{\ell j}/v \overline{\ell}_{Li}\ell_{Rj}$; only the right-handed tau lepton has a significant contribution. The induced $\Delta a_\mu$ is thus suppressed by the factor of $m_\mu^2 m_\tau / (v m_h^2)$ so that the value of $\Delta a_\mu$ is two orders of magnitude smaller than current data $\Delta a_\mu = a_\mu^{exp} - a_\mu^{SM} = (28.8 \pm 8.0) \times 10^{-10}$ [2]. A similar situation happens in $\tau \to 3\mu$ decay also. Since the couplings are suppressed by $m_\tau/v$ and $m_\mu/v$, the BR for $\tau \to 3\mu$ is of the order of $10^{-14}$. We also estimate the process $\tau \to \mu\gamma$ via the $h$-mediation. The effective interaction for $\tau \to \mu\gamma$ is expressed by

$$\mathcal{L}_{\tau \to \mu\gamma} = \frac{e}{16\pi^2} m_\tau \overline{\mu}\sigma_{\mu\nu}(C_L P_L + C_R P_R)\tau F^{\mu\nu}, \tag{26}$$
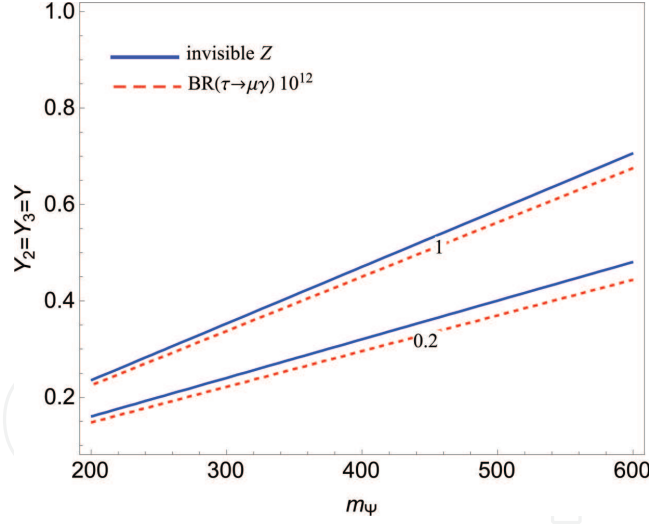
**Figure 1.**
*Contours for $BR(\tau \to \mu\gamma)$ (dashed) as a function of Y and $m_\Psi$, where the constraint from $\Gamma^Z_{inv}$ (solid) is included. (The plot is taken from ref. [29]).*

where $C_L = 0$ and the Wilson coefficient $C_R$ from the one loop is obtained as

$$C_R \approx \frac{C^h_{23} C^h_{33}}{2m^2_h} \left( \ln \frac{m^2_h}{m^2_\tau} - \frac{4}{3} \right). \tag{27}$$

Accordingly, the BR for $\tau \to \mu\gamma$ is expressed as

$$\frac{BR(\tau \to \mu\gamma)}{BR(\tau \to e\bar{\nu}_e\nu_\tau)} = \frac{3\alpha_e}{4\pi G^2_F} |C_R|^2. \tag{28}$$

We present the contours for $BR(\tau \to \mu\gamma)$ as a function of coupling Y and $m_\Psi$ in **Figure 1**, where the numbers on the plots are in units of $10^{-12}$. It can be seen that the resultant $BR(\tau \to \mu\gamma)$ can be only up to $10^{-12}$, where the current experimental upper bound is $BR(\tau \to \mu\gamma) < 4.4 \times 10^{-8}$ [2].

### 3.2 *B*-meson flavor physics with leptoquarks

This section is based on Ref. [32]. Several interesting excesses in semileptonic *B* decays have been observed in experiments such as (i) the angular observable $P'_5$ of $B \to K^*\mu^+\mu^-$ [7], where a $3\sigma$ deviation due to the integrated luminosity of 3.0 fb $^{-1}$ was found at the LHCb [8, 9], and the same measurement with a $2.6\sigma$ deviation was also confirmed by Belle [10] and (ii) the branching fraction ratios $R_{D,D^*}$, which are defined and measured as follows:

$$R_D = \frac{\overline{B} \to D\tau\nu}{\overline{B} \to D\ell\nu} = \begin{cases} 0.375 \pm 0.064 \pm 0.026 & \text{Belle [11],} \\ 0.440 \pm 0.058 \pm 0.042 & \text{BaBar [12, 13],} \end{cases}$$

$$R_{D^*} = \frac{\overline{B} \to D^*\tau\nu}{\overline{B} \to D^*\ell\nu} = \begin{cases} 0.302 \pm 0.030 \pm 0.011 & \text{Belle [14],} \\ 0.270 \pm 0.035 \pm^{+0.028}_{-0.025} & \text{Belle [15],} \\ 0.332 \pm 0.024 \pm 0.018 & \text{BaBar [12, 13],} \\ 0.336 \pm 0.027 \pm 0.030 & \text{LHCb [16],} \end{cases} \tag{29}$$

where $\ell = (e, \mu)$, and these measurements can test the violation of lepton flavor universality. The averaged results from the heavy flavor averaging group are $R_D = 0.403 \pm 0.040 \pm 0.024$ and $R_{D^*} = 0.310 \pm 0.015 \pm 0.008$ [35], and the SM predictions are around $R_D \approx 0.3$ [36, 37] and $R_{D^*} \approx 0.25$, respectively. Further tests of lepton flavor universality can be made using the branching fraction ratios: $R_{K^{(*)}} = BR(B \to K^{(*)} \mu^+ \mu^-)/BR(B \to K^{(*)} e^+ e^-)$. The current LHCb measurements are $R_K = 0.745^{+0.090}_{-0.074} \pm 0.036$ [38] and $R_{K^*} = 0.69^{+0.11}_{-0.07} \pm 0.05$ [39], which indicate a more than $2.5\sigma$ deviation from the SM prediction. Furthermore, a known anomaly is the muon anomalous magnetic dipole moment (muon $g - 2$), where its latest measurement is $\Delta a_\mu = a_\mu^{exp} - a_\mu^{SM} = (28.8 \pm 8.0) \times 10^{-10}$ [2]. These anomalies would be explained by introducing LQs and we review possible scenarios in the following.

### 3.2.1 Effective interactions for semileptonic B-decay

According to the interactions in Eq. (24), we first formulate the four-Fermi interactions for the $b \to c\ell' \bar{\nu}_{\ell'}$ and $b \to s\ell'^+ \ell'^-$ decays. For the $b \to c\ell' \bar{\nu}_{\ell'}$ processes, the induced current-current interactions from $k_{3j}\tilde{k}_{i2}$ and $\tilde{y}_{3i}w_{2j}$ are $(S - P) \times (S - P)$, and those from $y_{3j}y_{2j}$ and $\tilde{y}_{3i}\tilde{y}_{2j}$ are $(S - P) \times (S + P)$, where $S$ and $P$ denote the scalar and pseudoscalar currents, respectively. Taking the Fierz transformations, the Hamiltonian for the $b \to c\ell' \bar{\nu}_{\ell'}$ decays can be expressed as follows:

$$
\mathcal{H}_{b \to c} = \left( -\frac{\tilde{y}_{3i}w_{2j}}{2m_S^2} + \frac{k_{3j}\tilde{k}_{i2}}{2m_\Phi^2} \right) \bar{c} P_L b \, \bar{\ell}_j P_L \nu_i + \left( \frac{\tilde{y}_{3i}w_{2j}}{2m_S^2} + \frac{k_{3j}\tilde{k}_{i2}}{2m_\Phi^2} \right) \frac{1}{4} \bar{c} \sigma_{\mu\nu} P_L b \, \bar{\ell}_j \sigma^{\mu\nu} P_L \nu_i
$$
$$
- \sum_a V_{2a} \frac{y_{aj}y_{3i}}{4m_\Delta^2} \bar{c}\gamma_\mu P_L b \, \bar{\ell}_j \gamma^\mu P_L \nu_i + \sum_a V_{2a}\tilde{y}_{aj} \frac{\tilde{y}_{3i}}{2m_S^2} \bar{c}\gamma_\mu P_L b \, \bar{\ell}_j \gamma^\mu P_L \nu_i,
$$
$$(30)$$

where the indices $i, j$ are the lepton flavors and the LQs in the same representation are taken as degenerate particles in mass. It can be seen that the interaction structure obtained from the triplet LQ is the same as that from the $W$-boson one. The doublet LQ generates an $(S - P) \times (S - P)$ structure as well as a tensor structure. However, the singlet LQ can produce currents of $(V - A) \times (V - A)$, $(S - P) \times (S - P)$, and tensor structures. Nevertheless, we show later that the singlet LQ makes the main contribution to the $R_D$ and $R_{D^*}$ excesses. Note that it is difficult to explain $R_{D,D^*}$ by only using the doublet or/and triplet LQs when the $R_K$ excess and other strict constraints are satisfied at the same time.

With the Yukawa couplings in Eq. (24), the effective Hamiltonian for the $b \to s\ell'^+ \ell'^-$ decays mediated by $\phi^{2/3}$ and $\delta^{4/3}$ can be expressed as

$$
\mathcal{H}_{b \to s} = \frac{k_{3j}k_{2j}}{2m_\Phi^2} (\bar{s}\gamma^\mu P_L b)(\bar{\ell}_j \gamma_\mu P_R \ell_j),
$$
$$
- \frac{y_{3j}y_{2j}}{2m_\Delta^2} (\bar{s}\gamma^\mu P_L b)(\bar{\ell}_j \gamma_\mu P_L \ell_j),
$$
$$(31)$$

where the Fierz transformations have been applied. By Eq. (31), it can be clearly seen that the quark currents from both the doublet and triplet LQs are left-handed; however, the lepton current from the doublet (triplet) LQ is right(left)-handed. When one includes Eq. (31) in the SM contributions, the effective Hamiltonian for the $b \to s\ell'^+ \ell'^-$ decays is written as

$$\mathcal{H}_{b \to s} = \frac{G_F \alpha_{em} V_{tb} V_{ts}^*}{\sqrt{2}\pi} \left[ H_{1\mu} L^\mu + H_{2\mu} L^{5\mu} \right], \tag{32}$$

where the leptonic currents are denoted by $L_\mu^{(5)} = \bar{\ell} \gamma_\mu (\gamma_5) \ell$, and the related hadronic currents are defined as

$$H_{1\mu} = C_9^\ell \bar{s} \gamma_\mu P_L b - \frac{2m_b}{q^2} C_7 \bar{s} i \sigma_{\mu\nu} q^\nu P_R b,$$
$$H_{2\mu} = C_{10}^\ell \bar{s} \gamma_\mu P_L b. \tag{33}$$

The effective Wilson coefficients with LQ contributions are expressed as

$$C_{9(10)}^\ell = C_{9(10)}^{SM} + C_{9(10)}^{LQ,\ell'},$$
$$C_9^{LQ,\ell_j} = -\frac{1}{4c_{SM}} \left( \frac{k_{3j} k_{2j}}{m_\Phi^2} - \frac{y_{3j} y_{2j}}{m_\Delta^2} \right),$$
$$C_{10}^{LQ,\ell_j} = -\frac{1}{4c_{SM}} \left( \frac{k_{3j} k_{2j}}{m_\Phi^2} + \frac{y_{3j} y_{2j}}{m_\Delta^2} \right), \tag{34}$$

where $c_{SM} = V_{tb} V_{ts}^* \alpha_{em} G_F / (\sqrt{2}\pi)$ and $V_{ij}$ is the CKM matrix element. From Eq. (34), it can be seen that when the magnitude of $C_{10}^{LQ,\ell_j}$ is decreased, $C_9^{LQ,\ell_j}$ can be enhanced. That is, the synchrony of the increasing/decreasing Wilson coefficients of $C_9^{NP}$ and $C_{10}^{NP}$ from new physics is diminished in this model. In addition, the sign of $C_9^{LQ,\ell'}$ can be different from that of $C_{10}^{LQ,\ell'}$. As a result, when the constraint from $B_s \to \mu^+ \mu^-$ decay is satisfied, we can have sizable values of $C_9^{LQ,\mu}$ to fit the anomalies of $R_K$ and angular observable in $B \to K^* \mu^+ \mu^-$. Although the LQs can contribute to the electromagnetic dipole operators, since the effects are through one-loop diagrams and are also small, the associated Wilson coefficient $C_7$ is mainly from the SM contributions.

### 3.2.2 Constraints from $\Delta F = 2$, radiative lepton flavor violating, $B^+ \to K^+ \nu \bar{\nu}$, $B_s \to \mu^+ \mu^-$, and $B_c \to \tau \nu$ processes

Before we analyze the muon $g - 2$, $R_{D^{(*)}}$, and $R_{K^{(*)}}$ problems, we examine the possible constraints due to rare decay processes. Firstly, we discuss the strict constraints from the $\Delta F = 2$ processes, such as $F - \overline{F}$ oscillation, where $F$ denotes the neutral pseudoscalar meson. Since $K - \overline{K}$, $D - \overline{D}$, and $B_d - \overline{B}_d$ mixings are involved, the first-generation quarks and the anomalies mentioned earlier are associated with the second- and third-generation quarks. Therefore, we can avoid the constraints by assuming that $k_{1\ell'} \approx \tilde{k}_{\ell'1} \approx y_{1\ell'} \approx \tilde{y}_{1\ell'} \approx w_{1i} \approx 0$ without affecting the analyses of $R_{D^{(*)}}$ and $R_{K^{(*)}}$. Thus, the relevant $\Delta F = 2$ process is $B_s - \overline{B}_s$ mixing, where $\Delta m_{B_s} = 2|\langle \overline{B}_s | \mathcal{H} | B_s \rangle|$ is induced from box diagrams, and the LQ contributions can be formulated as

$$\Delta m_{B_s} \approx \frac{C_{box}}{(4\pi)^2} \left[ \frac{5}{4} \left( \frac{\sum_{i=1}^3 y_{3i} y_{2i}}{m_\Delta} \right)^2 + \left( \frac{\sum_{i=1}^3 k_{3i} k_{2i}}{m_\Phi} \right)^2 \right]$$
$$+ \frac{C_{box}}{(4\pi)^2} \left[ \left( \frac{\sum_{i=1}^3 \tilde{y}_{3i} \tilde{y}_{2i}}{m_S} \right)^2 + 2 \frac{\left( \sum_{i=1}^3 y_{3i} \tilde{y}_{2i} \right) \left( \sum_{i=1}^3 \tilde{y}_{3i} y_{2i} \right)}{m_S^2 - m_\Delta^2} \ln \left[ \frac{m_S}{m_\Delta} \right] \right], \tag{35}$$

where $C_{\text{box}} = m_{B_s} f_{B_s}^2 / 3$, $f_{B_s} \approx 0.224$ GeV is the decay constant of $B_s$-meson [40], and the current measurement is $\Delta m_{B_s}^{exp} = 1.17 \times 10^{-11}$ GeV [2]. To satisfy the $R_{K^{(*)}}$ excess, the rough magnitude of LQ couplings is $|y_{3i} y_{2i}| \sim |k_{3i} k_{2i}| \sim 5 \times 10^{-3}$. Using our parameter values, it can be shown that the resulting $\Delta m_{B_s}$ agree with the current experimental data. However, $\Delta m_{B_s}$ can indeed constrain the parameters involved in the $b \to c\ell'\bar{\nu}_{\ell'}$ decays.

In addition to the muon $g - 2$, the introduced LQs can also contribute to the lepton flavor violating processes $\ell' \to \ell\gamma$, where the current upper bounds are $BR(\mu \to e\gamma) < 4.2 \times 10^{-13}$ and $BR(\tau \to e(\mu)\gamma) < 3.3(4.4) \times 10^{-8}$ [2], and they can strictly constrain the LQ couplings. To understand the constraints due to the $\ell' \to \ell\gamma$ decays, one expresses their branching ratios (BRs) such as

$$BR(\ell_b \to \ell_a \gamma) = \frac{48\pi^3 \alpha_{em} C_{ba}}{G_F^2 m_{\ell_b}^2} \left( |(a_R)_{ab}|^2 + |(a_L)_{ab}|^2 \right) \qquad (36)$$

with $C_{\mu e} \approx 1$, $C_{\tau e} \approx 0.1784$, and $C_{\tau\mu} \approx 0.1736$. $(a_R)_{ab}$ is written as

$$(a_R)_{ab} \approx \frac{3}{(4\pi)^2} \int d[X] \, m_t \left( F_{k\tilde{k}} - F_{w\tilde{y}} \right)_{ab}, \qquad (37)$$

where $\int [dX] \equiv \int dx dy dz (1 - x - y - z)$, $(a_L)_{ab}$ can be obtained from $(a_R)_{ab}$ by using $\left( F_{\alpha\beta}^\dagger \right)_{ab}$ instead of $\left( F_{\alpha\beta} \right)_{ab}$, and the function $F_{k\tilde{k}}$ is given by

$$\left( F_{k\tilde{k}} \right)_{ab} = (\mathbf{Vk})_{3b} \tilde{k}_{a3} \left( \frac{5}{3} \frac{x}{\Delta(m_t, m_\Phi)_{ab}} + \frac{2}{3} \frac{1-x}{\Delta(m_\Phi, m_t)_{ab}} \right),$$

$$\left( F_{w\tilde{y}} \right)_{ab} = w_{3b} (\mathbf{V\tilde{y}})_{3a} \left( \frac{1}{3} \frac{x}{\Delta(m_t, m_S)_{ab}} + \frac{2}{3} \frac{1-x}{\Delta(m_S, m_t)_{ab}} \right), \qquad (38)$$

$$\Delta(m_1, m_2)_{ab} \approx x m_1^2 + (y + z) m_2^2.$$

Note that $\mathbf{Vk}_{3b} \approx k_{3b}$ and $\mathbf{V\tilde{y}}_{3a} \approx \tilde{y}_{3a}$ are due to $V_{ub,cb} \ll V_{tb} \approx 1$. From Eq. (24), we can see that the doublet and singlet LQs can simultaneously couple to both left- and right-handed charged leptons, and the results are enhanced by $m_t$. Other LQ contributions are suppressed by $m_\ell$ due to the chirality flip in the external lepton legs, and thus they are ignored. Based on Eq. (37), the muon $g - 2$ can be obtained as

$$\Delta a_\mu \simeq - m_\mu (a_L + a_R)_{a=b=\mu}. \qquad (39)$$

As mentioned earlier, the singlet LQ does not contribute to $b \to s\ell'^+\ell^-$ at the tree level, but it can induce the $b \to s\nu\bar{\nu}$ process, where the current upper bound is $B^+ \to K^+ \nu\bar{\nu} < 1.6 \times 10^{-5}$, and the SM result is around $4 \times 10^{-6}$. Thus, $B^+ \to K^+ \nu\bar{\nu}$ can bound the parameters of $\tilde{y}_{3i} \tilde{y}_{2i}$. The four-Fermi interaction structure, which is induced by the LQ, is the same as that induced by the $W$-boson, so we can formulate the BR for $B^+ \to K^+ \nu\bar{\nu}$ as

$$BR(B^+ \to K^+ \nu\bar{\nu}) \approx \frac{1}{3} \left( \sum_{\ell'} |1 - r_{\ell'}|^2 \right) BR^{SM}(B^+ \to K^+ \nu\bar{\nu}), \qquad (40)$$

$$r_{\ell'} = \frac{1}{C_{SM}^\nu} \left( \frac{\tilde{y}_{3\ell'} \tilde{y}_{2\ell'}}{2 m_S^2} + \frac{y_{3\ell'} y_{2\ell'}}{4 m_\Delta^2} \right), \qquad C_{SM}^\nu = \frac{G_F V_{tb} V_{ts}^*}{\sqrt{2}} \frac{\alpha_{em}}{2\pi \sin^2\theta_W} X(x_t), \qquad (41)$$

where $x_t = m_t^2/m_W^2$ and $X(x_t)$ can be parameterized as $X(x_t) \approx 0.65 x_t^{0.575}$ [41]. According to Eq. (31), the LQs also contribute to $B_s \to \mu^+\mu^-$ process, where the BRs measured by LHCb [42] and prediction in the SM [43] are $BR(B_s \to \mu^+\mu^-)^{exp} = \left(3.0 \pm 0.6^{+0.3}_{-0.2}\right) \times 10^{-9}$ and $BR(B_s \to \mu^+\mu^-)^{SM} = (3.65 \pm 0.23) \times 10^{-9}$, respectively. The experimental data are consistent with the SM prediction, and in order to consider the constraint from $B_s \to \mu^+\mu^-$, we use the expression for the BR as [44].

$$\frac{\mathrm{BR}(B_s \to \mu^+\mu^-)}{\mathrm{BR}(B_s \to \mu^+\mu^-)^{SM}} = \left| 1 - 0.24 C_{10}^{LQ,\mu} \right|^2. \tag{42}$$

In addition to the $B^- \to D^{(*)}\tau\bar{\nu}$ decay, the induced effective Hamiltonian in Eq. (30) also contributes to the $B_c \to \tau\bar{\nu}$ process, where the allowed upper limit is $BR\left(B_c^- \to \tau\bar{\nu}\right) < 30\%$ [45]. According to previous results given by [45], we express the BR for $B_c \to \tau\bar{\nu}$ as

$$BR(B_c \to \tau\bar{\nu}_\tau) = \tau_{B_c} \frac{m_{Bc} m_\tau^2 f_{B_c}^2 G_F^2 |V_{cb}|^2}{8\pi} \left(1 - \frac{m_\tau^2}{m_{B_c}^2}\right)^2 \left| 1 + \varepsilon_L + \frac{m_{B_c}^2}{m_\tau(m_b + m_c)} \varepsilon_P \right|^2, \tag{43}$$

where $f_{B_c}$ is the $B_c$ decay constant, and the $\varepsilon_{L,P}$ in our model is given as

$$\varepsilon_L = \frac{\sqrt{2}}{4 G_F V_{cb}} \left[ -\sum_a V_{2a} \frac{y_{a3} y_{33}}{4 m_\Delta^2} + \sum_a V_{2a} \frac{\tilde{y}_{a3} \tilde{y}_{33}}{2 m_S^2} \right],$$

$$\varepsilon_P = \frac{\sqrt{2}}{4 G_F V_{cb}} \left[ \frac{\tilde{y}_{33} w_{23}}{2 m_S^2} - \frac{k_{33} \tilde{k}_{32}}{2 m_\Phi^2} \right].$$

Using $\tau_{B_c} \approx 0.507 \times 10^{-12}$ s, $m_{B_c} \approx 6.275$ GeV, $f_{B_c} \approx 0.434$ GeV [46], and $V_{cb} \approx 0.04$, the SM result is $BR^{SM}(B_c \to \tau\bar{\nu}_\tau) \approx 2.1\%$. One can see that the effects of the new physics can enhance the $B_c \to \tau\bar{\nu}_\tau$ decay by a few factors at most in our analysis.

### 3.2.3 Observables: $R_{D^{(*)}}$ and $R_{K^{(*)}}$

The observables of $R_{D^{(*)}}$ and $R_{K^{(*)}}$ are the branching fraction ratios that are insensitive to the hadronic effects giving clearer test of lepton universality in $B$-meson decay, but the associated BRs still depend on the transition form factors. In order to calculate the BR for each semileptonic decay process, we parameterize the transition form factors for $\bar{B} \to P$ by

$$\langle P(p_2)|q\gamma^\mu b|\bar{B}(p_1)\rangle = F_+(q^2)\left( (p_1 + p_2)^\mu - \frac{m_B^2 - m_P^2}{q^2} q^\mu \right) + \frac{m_B^2 - m_P^2}{q^2} q^\mu F_0(q^2),$$

$$\langle P(p_2)|q\sigma_{\mu\nu} b|\bar{B}(p_1)\rangle = -i\left( p_{1\mu} p_{2\nu} - p_{1\nu} p_{2\mu} \right) \frac{2 F_T(q^2)}{m_B + m_P}, \tag{44}$$

where $P$ can be the $D(q = c)$ or $K(q = s)$ meson and the momentum transfer is given by $q = p_1 - p_2$. For the $B \to V$ decay where $V$ is a vector meson, the transition form factors associated with the weak currents are parameterized such that

$$\langle V(p_2, \varepsilon)|\bar{q}\gamma_\mu b|\overline{B}(p_1)\rangle = i\varepsilon_{\mu\nu\rho\sigma}\varepsilon^{\nu*}p_1^\rho p_2^\sigma \frac{2V(q^2)}{m_B + m_V},$$

$$\langle V(p_2, \varepsilon)|\bar{q}\gamma_\mu\gamma_5 b|\overline{B}(p_1)\rangle = 2m_V A_0(q^2)\frac{\varepsilon^* \cdot q}{q^2}q_\mu + (m_B + m_V)A_1(q^2)\left(\varepsilon_\mu^* - \frac{\varepsilon^* \cdot q}{q^2}q_\mu\right)$$

$$- A_2(q^2)\frac{\varepsilon^* \cdot q}{m_B + m_V}\left((p_1 + p_2)_\mu - \frac{m_B^2 - m_V^2}{q^2}q_\mu\right),$$

$$\langle V(p_2, \varepsilon)|\bar{q}\sigma_{\mu\nu}b|\overline{B}(p_1)\rangle = \varepsilon_{\mu\nu\rho\sigma}\left[\varepsilon^{\rho*}(p_1 + p_2)^\sigma T_1(q^2) + \varepsilon^{\rho*}q^\sigma\frac{m_B^2 - m_V^2}{q^2}(T_2(q^2) - T_1(q^2))\right.$$

$$\left.+ 2\frac{\varepsilon^* \cdot q}{q^2}p_1^\rho p_2^\sigma\left(T_2(q^2) - T_1(q^2) + \frac{q^2}{m_B^2 - m_V^2}T_3(q^2)\right)\right],$$

$$(45)$$

where $V = D^*(K^*)$ when $q = c(s)$, $\varepsilon^{0123} = 1$, $\sigma_{\mu\nu}\gamma_5 = (i/2)\varepsilon_{\mu\nu\rho\sigma}\sigma^{\rho\sigma}$, and $\varepsilon^\mu$ is the polarization vector of the vector meson. Here we note that the form factors associated with the weak scalar/pseudoscalar currents can be obtained through the equations of motion, i.e., $i\partial_\mu\bar{q}\gamma^\mu b = (m_b - m_q)\bar{q}b$ and $i\partial_\mu(\bar{q}\gamma^\mu\gamma_5 b) = -(m_b + m_q)\bar{q}\gamma_5 b$. For numerical estimations, the $q^2$-dependent form factors $F_+$, $F_T$, $V$, $A^0$, and $T_1$ are taken as [47]

$$f(q^2) = \frac{f(0)}{\left(1 - q^2/M^2\right)\left(1 - \sigma_1 q^2/M^2 + \sigma_2 q^4/M^4\right)}, \qquad (46)$$

and the other form factors are taken to be

$$f(q^2) = \frac{f(0)}{1 - \sigma_1 q^2/M^2 + \sigma_2 q^4/M^4}. \qquad (47)$$

The values of $f(0)$, $\sigma_1$, and $\sigma_2$ for each form factor are summarized in **Table 2**. A detailed discussion of the form factors can be referred to [47]. The next-to-next-leading (NNL) effects obtained with the LCQCD Some Rule approach for the $B \to D$ form factors were described by [48].

According to the form factors in Eqs. (44) and (45), and the interactions in Eqs. (30) and (32), we briefly summarize the differential decay rates for the semileptonic $B$ decay processes, which we use for estimating $R_{D^{(*)}}$ and $R_K$. For the $\overline{B} \to D\ell'\bar{\nu}_{\ell'}$ decay, the differential decay rate as a function of the invariant mass $q^2$ can be given by

| | $B \to D$ | | | $B \to D^*$ | | | | | | |
|---|---|---|---|---|---|---|---|---|---|---|
| | $F_+$ | $F_0$ | $F_T$ | $V$ | $A_0$ | $A_1$ | $A_2$ | $T_1$ | $T_2$ | $T_3$ |
| f(0) | 0.67 | 0.67 | 0.69 | 0.76 | 0.69 | 0.66 | 0.62 | 0.68 | 0.68 | 0.33 |
| $\sigma_1$ | 0.57 | 0.78 | 0.56 | 0.57 | 0.58 | 0.78 | 1.40 | 0.57 | 0.64 | 1.46 |
| $\sigma_2$ | | | | | | | 0.41 | | | |
| | $B \to K$ | | | $B \to K^*$ | | | | | | |
| f(0) | 0.36 | 0.36 | 0.35 | 0.44 | 0.45 | 0.36 | 0.32 | 0.39 | 0.39 | 0.27 |
| $\sigma_1$ | 0.43 | 0.70 | 0.43 | 0.45 | 0.46 | 0.64 | 1.23 | 0.45 | 0.72 | 1.31 |
| $\sigma_2$ | | 0.27 | | | | 0.36 | 0.38 | | 0.62 | 0.41 |

**Table 2.**
*$B \to P, V$ transition form factors, as parameterized in Eqs. (46) and (47).*

$$\frac{d\Gamma_D^{\ell'}}{dq^2} = \frac{G_F^2 |V_{cb}|^2 \sqrt{\lambda_D}}{256\pi^3 m_B^3} \left(1 - \frac{m_{\ell'}^2}{q^2}\right)^2 \left[\frac{2}{3}\left(2 + \frac{m_{\ell'}^2}{q^2}\right)|X_+^{\ell'}|^2 + \frac{2m_{\ell'}^2}{q^2}\left|X_0^{\ell'} + \frac{\sqrt{q^2}}{m_{\ell'}}X_S^{\ell'}\right|^2\right.$$

$$\left. + 16\left(\frac{2}{3}\left(1 + \frac{2m_{\ell'}^2}{q^2}\right)|X_T^{\ell'}|^2 - \frac{m_{\ell'}}{\sqrt{q^2}}X_T^{\ell'}X_0^{\ell'}\right)\right],$$

$$(48)$$

where the $\left\{X_\alpha^{\ell'}\right\}$ functions and LQ contributions are

$$X_+^{\ell'} = \sqrt{\lambda_D}\left(1 + C_V^{\ell'}\right)F_+(q^2), \quad X_0^{\ell'} = (m_B^2 - m_D^2)\left(1 + C_V^{\ell'}\right)F_0(q^2)$$

$$X_S^{\ell'} = \frac{m_B^2 - m_D^2}{m_b - m_c}C_S^{\ell'}\sqrt{q^2}F_0(q^2), \quad X_T^{\ell'} = -\frac{\sqrt{q^2\lambda_D}}{m_B + m_D}C_T^{\ell'}F_T(q^2)$$

$$C_V^{\ell'} = \frac{\sqrt{2}}{8G_F V_{cb}}\sum_a V_{2a}\left(\frac{\tilde{y}_{3\ell'}\tilde{y}_{a\ell'}}{m_S^2} - \frac{y_{3\ell'}y_{a\ell'}}{2m_\Delta^2}\right),$$

$$C_S^{\ell'} = -\frac{\sqrt{2}}{4G_F V_{cb}}\left(\frac{\tilde{y}_{3\ell'}w_{2\ell'}}{2m_S^2} - \frac{k_{3\ell'}\tilde{k}_{\ell'2}}{2m_\Phi^2}\right), \quad C_T^{\ell'} = \frac{\sqrt{2}}{16G_F V_{cb}}\left(\frac{\tilde{y}_{3\ell'}w_{2\ell'}}{2m_S^2} + \frac{k_{3\ell'}\tilde{k}_{\ell'2}}{2m_\Phi^2}\right),$$

$$\lambda_H = m_B^4 + m_H^4 + q^4 - 2(m_B^2 m_H^2 + m_H^2 q^2 + q^2 m_B^2).$$

$$(49)$$

We note that the effective couplings $C_S^{\ell'}$ and $C_T^{\ell'}$ at the $m_b$ scale can be obtained from the LQ mass scale via the renormalization group (RG) equation. Our numerical analysis considers the RG running effects with $\left(C_S^{\ell'}/C_T^{\ell'}\right)_{\mu=m_b}/\left(C_S^{\ell'}/C_T^{\ell'}\right)_{\mu=\mathcal{O}(TeV)} \sim 2.0$ at the $m_b$ scale [49]. The $\bar{B} \to D^*\ell'\bar{\nu}_{\ell'}$ decays involve $D^*$ polarizations and more complicated transition form factors, so the differential decay rate determined by summing all of the $D^*$ helicities are

$$\frac{d\Gamma_{D^*}^{\ell'}}{dq^2} = \sum_{h=L,+,-}\frac{d\Gamma_{D^*}^{\ell'h}}{dq^2} = \frac{G_F^2 |V_{cb}|^2 \sqrt{\lambda_{D^*}}}{256\pi^3 m_B^3}\left(1 - \frac{m_{\ell'}^2}{q^2}\right)^2 \sum_{h=L,+,-}V_{D^*}^{\ell'h}(q^2), \qquad (50)$$

where $\lambda_{D^*}$ is found in Eq. (53) and the detailed $\left\{V_{D^*}^{\ell'h}\right\}$ functions are shown in the appendix. According to Eqs. (48) and (50), $R_M$ ($M = D, D^*$) can be calculated by

$$R_M = \frac{\int_{m_\tau^2}^{q_{\max}^2}dq^2\left(d\Gamma_M^\tau/dq^2\right)}{\int_{m_\ell^2}^{q_{\max}^2}dq^2\left(d\Gamma_M^\ell/dq^2\right)} \qquad (51)$$

where $q_{\max}^2 = (m_B - m_M)^2$ and $\Gamma_M^\ell = \left(\Gamma_M^e + \Gamma_M^\mu\right)/2$. For the $B \to K\ell^+\ell^-$ decays, the differential decay rate can be expressed as [50].

$$\frac{d\Gamma_{K\ell\ell}(q^2)}{dq^2} \approx \frac{|c_{SM}|^2 m_B^3}{3 \cdot 2^8 \pi^3}\left(1 - \frac{q^2}{m_B^2}\right)^{3/2}$$

$$\times \left[\left|C_9^\ell F_+(q^2) + \frac{2m_b C_7}{m_B + m_K}F_T(q^2)\right|^2 + |C_{10}^\ell F_+(q^2)|^2\right]. \qquad (52)$$

From Eq. (52), the measured ratio $R_K$ in the range $q^2 = \left[q^2_{\min}, q^2_{\max}\right] = [1, 6]\ \text{GeV}^2$ can be estimated by

$$R_K = \frac{\int_{q^2_{\min}}^{q^2_{\max}} dq^2 d\Gamma_{K\mu\mu}/dq^2}{\int_{q^2_{\min}}^{q^2_{\max}} dq^2 d\Gamma_{Kee}/dq^2}. \tag{53}$$

$R_{K^*}$ is similar to $R_K$, and thus we only show the result for $R_K$.

### 3.2.4 Numerical analysis

After discussing the possible constraints and observables of interest, we now present the numerical analysis to determine the common parameter region where the $R_{D^{(*)}}$ and $R_{K^{(*)}}$ anomalies can fit the experimental data. Before presenting the numerical analysis, we summarize the relevant parameters, which are related to the specific measurements as follows:

$$\begin{aligned}
\text{muon } g - 2 &: k_{32}\tilde{k}_{23}, \tilde{y}_{32}w_{32}; \quad R_K : k_{3\ell}k_{2\ell}, y_{3\ell}y_{2\ell}; \\
R_{D^{(*)}} &: k_{3\ell'}\tilde{k}_{\ell'2}, \sum_a V_{2a}\big(y_{3\ell'}y_{a\ell'}, \tilde{y}_{3\ell'}\tilde{y}_{a\ell'}\big), \tilde{y}_{3\ell'}w_{2\ell'}.
\end{aligned} \tag{54}$$

The parameters related to the radiative LFV, $\Delta B = 2$, and $B^+ \to K^+ \nu\bar{\nu}$ processes are defined as

$$\begin{aligned}
\mu \to e\gamma &: k_{32}\tilde{k}_{13}, \tilde{k}_{23}k_{31}, \tilde{y}_{32}w_{31}, w_{32}\tilde{y}_{31}; \\
\tau \to \ell_a\gamma &: k_{33}\tilde{k}_{a3}, \tilde{k}_{33}k_{3a}, \tilde{y}_{33}w_{3a}, w_{33}\tilde{y}_{3a}; \\
B^+ \to K^+\nu\bar{\nu} &: \tilde{y}_{3i}\tilde{y}_{2i}, y_{3i}y_{2i}; \quad B_s \to \mu^+\mu^- : k_{32}k_{22}, y_{32}y_{22}; \\
\Delta m_{B_s} &: \left(\sum_i z_{3i}z_{2i}\right)^2, \left(\sum_i y_{3i}\tilde{y}_{2i}\right)\left(\sum_i \tilde{y}_{3i}y_{2i}\right),
\end{aligned} \tag{55}$$

where $z_{3i}z_{2i} = k_{3i}k_{2i}, y_{3i}y_{2i}, \tilde{y}_{3i}\tilde{y}_{2i}$. From Eqs. (54) and (55), we can see that in order to avoid the $\mu \to e\gamma$ and $\tau \to \ell\gamma$ constraints and obtain a sizable and positive $\Delta a_\mu$, we can set $(\tilde{k}_{13,33}, k_{31,33}, w_{3i})$ as a small value. From the upper limit of $B^+ \to K^+\nu\bar{\nu}$, we obtain $\tilde{y}_{3i}\tilde{y}_{2i} < 0.03$, and thus the resulting $\Delta m_{B_s}$ is smaller than the current data. In order to further suppress the number of free parameters and avoid large fine-tuning of couplings, we employ the scheme with $k_{ij} \approx \tilde{k}_{ji} \approx |y_{ij}|$, where the sign of $y_{ij}$ can be selected to obtain the correct sign for $C_9^{LQ, \ell_j}$ and to decrease the value of $C_{10}^{LQ, \mu}$ so that $B_s \to \mu^+\mu^-$ can fit the experimental data. As mentioned above, to avoid the bounds from the $K$, $B_d$, and $D$ systems, we also adopt $k_{1\ell'} \approx \tilde{k}_{\ell'1} \approx y_{1i} \approx \tilde{y}_{1i} \approx w_{1i} \sim 0$. When we omit these small coupling constants, the correlations of the parameters in Eqs. (54) and (55) can be further simplified as

$$\begin{aligned}
\text{muon } g - 2 &: k_{32}\tilde{k}_{23}; \quad R_K : k_{32}k_{22}, \ y_{32}y_{22}; R_{D^{(*)}} : k_{32}k_{22}, y_{32}y_{22}, \tilde{y}_{3\ell'}w_{2\ell'}; \\
B_s \to \mu^+\mu^- &: k_{32}k_{22}, y_{32}y_{22}; \quad \Delta m_{B_s} : (k_{32}k_{22})^2, (y_{32}y_{22})^2,
\end{aligned} \tag{56}$$

where $\tilde{y}_{3i}\tilde{y}_{2i}$ are ignored due to the constraint from $B^+ \to K^+\nu\bar{\nu}$. The typical values of these parameters for fitting the anomalies in the $b \to s\mu^+\mu^-$ decay are $y_{32}(k_{32}), y_{22}(k_{22}) \sim 0.07$, so the resulting $\Delta m_{B_s}$ is smaller than the current data, but

these parameters are too small to explain $R_{D^{(*)}}$. Thus, we must depend on the singlet LQ to resolve the $R_D$ and $R_{D^*}$ excesses, where as main free parameters are now $\tilde{y}_{3\ell'} w_{2\ell'}$.

After discussing the constraints and the correlations among various processes, we present the numerical analysis. There are several LQs in this scenario, but we use $m_{LQ}$ to denote the mass of all LQs. From Eqs. (37), (39), and (56), we can see that the muon $g - 2$ depends only on $k_{32}\tilde{k}_{23}$ and $m_\Phi$. Here we illustrate $\Delta a_\mu$ as a function of $k_{32}\tilde{k}_{23}$ in **Figure 2(a)**, where the solid, dashed, and dotted lines denote the results for $m_\Phi = 1.5, 5$, and 10 TeV, respectively, and the band is the experimental value with $1\sigma$ errors. Due to the $m_t$ enhancement, $k_{32}\tilde{k}_{23} \sim 0.05$ with $m_\Phi \sim 1$ TeV can explain the muon $g - 2$ anomaly.

According to the relationships shown in Eq. (56), $R_K$, $B_s \to \mu^+\mu^-$, and $\Delta m_{B_s}$ depend on the same parameters, i.e., $k_{32}k_{22}$ and $y_{32}y_{22}$. We show the contours for these observables as a function of $k_{32}k_{22}$ and $y_{32}y_{22}$ in **Figure 2(b)**, where the data with $1\sigma$ errors and $m_{LQ} = 1.5$ TeV are taken for all LQ masses. Based on these results, we see that $\Delta m_{B_s} < \Delta m_{B_s}^{exp}$ in the range of $|k_{32}k_{22}|$, $|y_{32}y_{22}| < 0.05$, where $R_K$ and $BR(B_s \to \mu^+\mu^-)$ can both fit the experimental data simultaneously. In addition, we show $C_9^{LQ,\mu} = [-1.5, -0.5]$ in the same plot. We can see that $C_9^{LQ,\mu} \sim -1$, which is used to explain the angular observable $P_5'$, can also be achieved in the same common region. According to **Figure 2(b)**, the preferred values of $k_{32}k_{22}$ and $y_{32}y_{22}$ where the observed $R_K$ and $B_s \to \mu^+\mu^-$ and the $C_9^{LQ,\mu} = [-1.5, -0.5]$ overlap are around $(k_{32}k_{22}, y_{32}y_{22}) \sim (-0.001, 0.004)$ and $\sim (0.025, 0.03)$. The latter values are at the percentage level, but they are still not sufficiently large to explain the tree-dominated $R_D$ and $R_{D^*}$ anomalies.

After studying the muon $g - 2$ and $R_K$ anomalies, we numerically analyze the ratio of $BR(\overline{B} \to D^{(*)}\tau\overline{\nu}_\tau)$ to $BR(\overline{B} \to D^{(*)}\ell\overline{\nu}_\ell)$, i.e., $R_{D^{(*)}}$. The introduced doublet and triplet LQs cannot efficiently enhance $R_{D^{(*)}}$, so in the following estimations, we only focus on the singlet LQ contributions, where the four-Fermi interactions shown in Eq. (30) come mainly from the scalar- and tensor-type interaction structures. Based
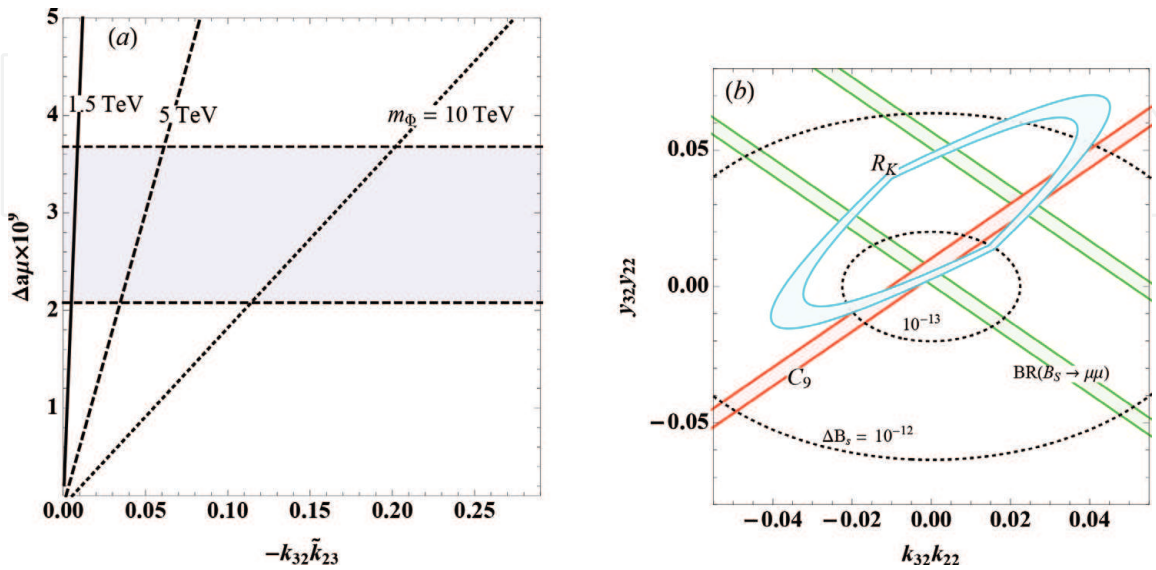


**Figure 2.**
*(a) $\Delta a_\mu$ as a function of $k_{32}\tilde{k}_{23}$ with $m_\Phi = 1.5, 5, 10$ TeV, where the band denotes the experimental data with $1\sigma$ errors. (b) Contours for $R_K$, $B_s \to \mu^+\mu^-$, $\Delta m_{B_s}$, and $C_9^{LQ,\mu}$ as a function of $k_{32}k_{22}$ and $y_{32}y_{22}$, where the ranges of $R_K$ and $B_s \to \mu^+\mu^-$ are the experimental values with $1\sigma$ errors and $m_{LQ} = 1.5$ TeV. For $C_9^{LQ,\mu}$, we show the range for $C^{LQ,\mu} = [-1.5, -0.5]$. (These plots are taken from Ref. [32]).*

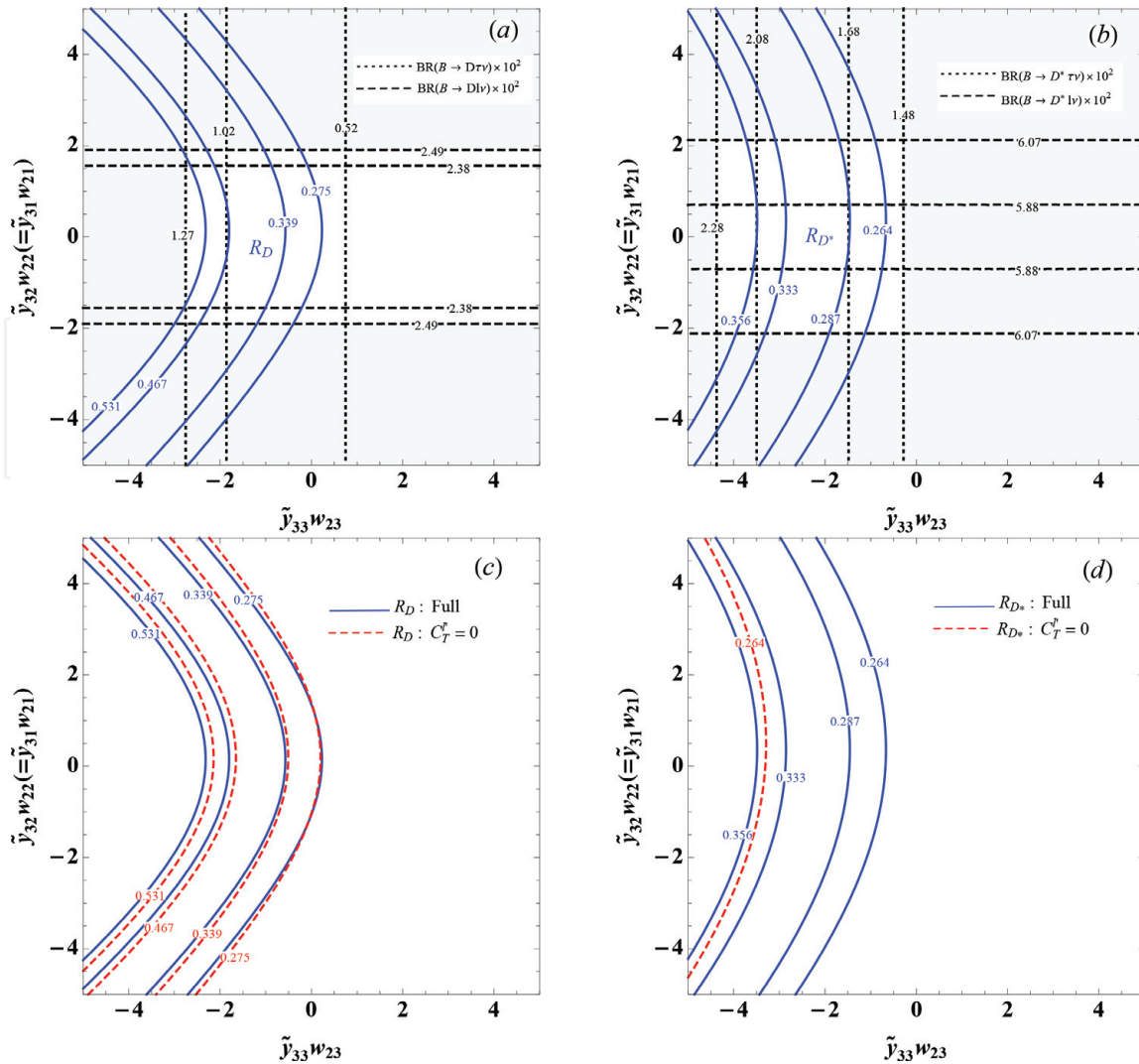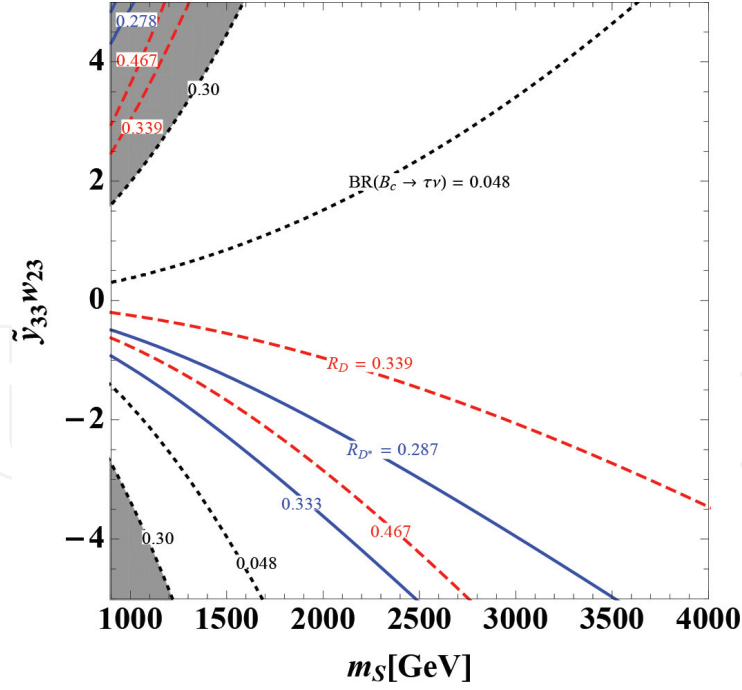**Figure 3.**
*Contours for (a) $R_D$ and (b) $R_{D^*}$, where the solid lines denote the data with $1\sigma$ and $2\sigma$ errors, respectively. The horizontal dashed lines in both plots denote the $BR^{exp}(B^+ \to D^{(*)}\ell\nu_\ell)$, whereas the vertical dotted lines are the $BR^{exp}(B^+ \to D^{(*)}\tau\nu_\tau)$. Contours for (c) $R_D$ and (d) $R_{D^*}$, where the solid and dashed lines denote the situations with and without tensor operator contributions, respectively. In this case, we take $m_{LQ} = 1.5$ TeV. (These plots are taken from ref. [32]).*

on Eqs. (48), (50), and (51), we show the contours for $R_D$ and $R_{D^*}$ as a function of $\tilde{y}_{33}w_{23}$ and $\tilde{y}_{32}w_{22}(\tilde{y}_{31}w_{21})$ in **Figure 3(a)** and **(b)**, where the horizontal dashed and vertical dotted lines in both plots denote $BR^{exp}(B^- \to D[\ell\nu_\ell, \tau\nu_\tau]) = [2.27 \pm 0.11, 0.77 \pm 0.25]\%$ and $BR^{exp}(B^- \to D^*[\ell\nu_\ell, \tau\nu_\tau]) = [5.69 \pm 0.19, 1.88 \pm 0.20]\%$, respectively, and $m_{LQ} = 1.5$ TeV is used, and the data with $2\sigma$ errors are taken. For simplicity, we take $\tilde{y}_{31}w_{21} \approx \tilde{y}_{32}w_{22}$. When considering the limits from $BR(\overline{B} \to D^{(*)}\ell'\overline{\nu}_{\ell'})$, we obtain the limits $|\tilde{y}_{3\ell}w_{2\ell}| \lesssim 1.5$ and $\tilde{y}_{33}w_{23} > 0$. In order to clearly demonstrate the influence of tensor-type interactions, we also calculate the situation by setting $C_T^{\ell'} = 0$. The contours obtained for $R_D$ and $R_{D^*}$ are shown in **Figure 3(c)** and **(d)**, where the solid and dashed lines denote the cases with and without $C_T^{\ell'}$, respectively. According to these plots, we can see that $R_D$ and $R_{D^*}$ have different responses to the tensor operators, where the latter is more sensitive to the tensor interactions. $R_D$ and $R_{D^*}$ can be explained simultaneously with the tensor couplings. In order to understand the correlation between $BR(B_c \to \tau\overline{\nu}_\tau)$ and $R_{D^{(*)}}$, we show the contours for $BR(B_c \to \tau\overline{\nu}_\tau)$ and $R_{D^{(*)}}$ as a function of $w_{23}\tilde{y}_{33}$ and $m_S$ in **Figure 4**, where $\tilde{y}_{32}w_{22} \approx \tilde{y}_{31}w_{21} \approx 0$ are used, and the gray area is excluded by

**Figure 4.**
*Contours for $BR(B_c \to \tau\bar{\nu}_\tau)$ and $R_{D^{(*)}}$ as a function of $w_{23}\tilde{y}_{23}$ and $m_S$. (The plot is taken from ref. [32]).*

$BR\left(B_c^- \to \tau\nu\right) < 0.3$. We can see that the predicted $BR(B_c \to \tau\bar{\nu}_\tau)$ is much smaller than the experimental bound.

Finally, we make some remarks regarding the constraint due to the LQ search at the LHC. Due to the flavor physics constraints, only the $S^{1/3}$ Yukawa couplings $\tilde{y}_{t\tau}$, $\tilde{y}_{b\nu_\tau}$, and $w_{c\tau}$ can be of $O(1)$. These couplings affect the $S^{1/3}$ decays but also their production. Therefore, in addition to the $S^{1/3}$-pair production, based on the $O(1)$ Yukawa couplings, the single $S^{1/3}$ production becomes interesting. In the $pp$ collisions, the single $S^{1/3}$ production can be generated via the $gb \to S^{-1/3}\bar{\nu}_\tau$ and $gc \to S^{-1/3}\tau^+$ channels. Using CalcHEP 3.6 [51, 52] with the CTEQ6 parton distribution functions [53], their production cross sections with $|w_{23}| \sim |\tilde{y}_{b\nu_\tau}| \sim \sqrt{2}$ and $m_{LQ} = 1000$ GeV at $\sqrt{s} = 13$ TeV can be obtained as 3.9 fb and 2.9 fb, respectively, whereas the $S^{1/3}$-pair production cross section is $\sigma\left(pp \to S^{-1/3}S^{1/3}\right) \approx 2.4$ fb. If we assume that $S^{-1/3}$ predominantly decays into $t\tau$, $b\nu_\tau$, and $c\tau$ with similar BRs, i.e. $BR\left(S^{-1/3} \to f\right) \sim 1/3$, then the single $S^{1/3}$ production cross section $\sigma\left(S^{-1/3}X\right)$ times $BR\left(S^{-1/3} \to f\right)$ with $X$ and $f$ as the possible final states can be estimated as around 1 fb. The LQ coupling $w_{23}$ involves different generations, so the constraints due to the collider measurements may not be applied directly. However, if we compare this with the CMS experiment [54] based on a single production of the second-generation scalar LQ, we find that the values of $\sigma \times BR$ at $m_{LQ} \sim 1000$ GeV are still lower than the CMS upper limit with few fb. The significance of this discovery depends on the kinematic cuts and event selection conditions, but this discussion is beyond the scope of this study, and we leave the detailed analysis for future research.

## 4. Conclusions

We have reviewed some charged particles which appear from physics beyond the Standard Model of particle physics. Some possible candidates of them are listed

such as charged scalar boson, vector-like leptons, vector-like quarks, and leptoquarks. After showing some properties and interactions of these particles, we reviewed some applications to flavor physics in which lepton flavor physics with vector-like lepton and *B*-meson physics with leptoquarks are focused on as an illumination. We have seen rich phenomenology that would be induced from such new charged particles, and they will be also tested in the future experiments.

## Author details

Takaaki Nomura
School of Physics, Korea Institute for Advanced Study, Seoul, Republic of Korea

*Address all correspondence to: nomura@kias.re.kr

IntechOpen

# References

[1] Bennett GW et al. [Muon g-2 Collaboration]. Final report of the muon E821 anomalous magnetic moment measurement at BNL. Physical Review D. 2006;**73**:072003. DOI: 10.1103/PhysRevD.73.072003. [hep-ex/0602035]

[2] Patrignani C et al. [Particle Data Group]. Review of particle physics. Chinese Physics C. 2016;**40**(10): 100001. DOI: 10.1088/1674-1137/40/10/100001

[3] Davier M, Hoecker A, Malaescu B, Zhang Z. Reevaluation of the hadronic contributions to the muon g-2 and to alpha (MZ). European Physical Journal C: Particles and Fields. 2011;**71**:1515. DOI: 10.1140/epjc/s10052-010-1515-z; Erratum: European Physical Journal C: Particles and Fields. 2012;**72**:1874. DOI: 10.1140/epjc/s10052-012-1874-8. [arXiv:1010.4180 [hep-ph]]

[4] Jegerlehner F, Szafron R. $\rho^0 - \gamma$ mixing in the neutral channel pion form factor $F_\pi^e$ and its role in comparing $e^+e^-$ with $\tau$ spectral functions. European Physical Journal C: Particles and Fields. 2011;**71**:1632. DOI: 10.1140/epjc/s10052-011-1632-3. [arXiv:1101.2872 [hep-ph]]

[5] Hagiwara K, Liao R, Martin AD, Nomura D, Teubner T. (g-2)$\mu$ and alpha ($M\_Z^2$) re-evaluated using new precise data. Journal of Physics G. 2011;**38**: 085003. DOI: 10.1088/0954-3899/38/8/085003. [arXiv:1105.3149 [hep-ph]]

[6] Aoyama T, Hayakawa M, Kinoshita T, Nio M. Complete tenth-order QED contribution to the muon g-2. Physical Review Letters. 2012;**109**:111808. DOI: 10.1103/PhysRevLett.109.111808. [arXiv:1205.5370 [hep-ph]]

[7] Descotes-Genon S, Matias J, Ramon M, Virto J. Implications from clean observables for the binned analysis of $B - > K*\mu^+\mu^-$ at large recoil. JHEP. 2013;**1301**:048. DOI: 10.1007/JHEP01(2013)048. [arXiv:1207.2753 [hep-ph]]

[8] Aaij R et al. [LHCb Collaboration]. Angular analysis of the $B^0 \rightarrow K^{*0}\mu^+\mu^-$ decay using 3 fb$^{-1}$ of integrated luminosity. JHEP. 2016;**1602**:104. DOI: 10.1007/JHEP02(2016)104. [arXiv:1512.04442 [hep-ex]]

[9] Aaij R et al. [LHCb Collaboration]. Measurement of form-factor-independent observables in the decay $B^0 \rightarrow K^{*0}\mu^+\mu^-$. Physical Review Letters. 2013;**111**:191801. DOI: 10.1103/PhysRevLett.111.191801. [arXiv:1308.1707 [hep-ex]]

[10] Wehle S et al. [Belle Collaboration]. Lepton-Flavor-Dependent Angular Analysis of $B \rightarrow K^*\ell^+\ell^-$. Physical Review Letters. 2017;**118**(11):111801. DOI: 10.1103/PhysRevLett.118.111801 [arXiv:1612.05014 [hep-ex]]

[11] Huschle M et al. [Belle Collaboration]. Measurement of the branching ratio of $\overline{B} \rightarrow D^{(*)}\tau^-\overline{\nu}_\tau$ relative to $\overline{B} \rightarrow D^{(*)}\ell^-\overline{\nu}_\ell$ decays with hadronic tagging at Belle. Physical Review D. 2015;**92**(7):072014. DOI: 10.1103/PhysRevD.92.072014. [arXiv:1507.03233 [hep-ex]]

[12] Lees JP et al. [BaBar Collaboration]. Evidence for an excess of $\overline{B} \rightarrow D^{(*)}\tau^-\overline{\nu}_\tau$ decays. Physical Review Letters. 2012; **109**:101802. DOI: 10.1103/PhysRevLett.109.101802. [arXiv:1205.5442 [hep-ex]]

[13] Lees JP et al. [BaBar Collaboration]. Measurement of an excess of $\overline{B} \rightarrow D^{(*)}\tau^-\overline{\nu}_\tau$ decays and implications for charged Higgs bosons. Physical Review D. 2013;**88**(7):072012. DOI: 10.1103/PhysRevD.88.072012. [arXiv:1303.0571 [hep-ex]]

[14] Abdesselam A et al. [Belle Collaboration]. Measurement of the branching ratio of $\overline{B}^0 \to D^{*+}\tau^-\overline{\nu}_\tau$ relative to $\overline{B}^0 \to D^{*+}\ell^-\overline{\nu}_\ell$ decays with a semileptonic tagging method. arXiv: 1603.06711 [hep-ex]

[15] Hirose S et al. [Belle Collaboration]. Measurement of the $\tau$ lepton polarization and $R(D^*)$ in the decay $\overline{B} \to D^*\tau^-\overline{\nu}_\tau$. Physical Review Letters. 2017;**118**(21):211801. DOI: 10.1103/PhysRevLett.118.211801. [arXiv: 1612.00529 [hep-ex]]

[16] Aaij R et al. [LHCb Collaboration]. Measurement of the ratio of branching fractions $\mathcal{B}\left(\overline{B}^0 \to D^{*+}\tau^-\overline{\nu}_\tau\right) / \mathcal{B}\left(\overline{B}^0 \to D^{*+}\mu^-\overline{\nu}_\mu\right)$. Physical Review Letters. 2015;**115**(11):111803. DOI: 10.1103/PhysRevLett.115.111803; Addendum: Physical Review Letters. 2015;**115**(15):159901. DOI: 10.1103/PhysRevLett.115.159901. [arXiv: 1506.08614 [hep-ex]]

[17] Gunion JF, Haber HE, Kane GL, Dawson S. The Higgs hunter's guide front. Physiologie. 2000;**80**:1

[18] Branco GC, Ferreira PM, Lavoura L, Rebelo MN, Sher M, Silva JP. Theory and phenomenology of two-Higgs-doublet models. Physics Reports. 2012;**516**:1. DOI: 10.1016/j.physrep.2012.02.002. [arXiv:1106.0034 [hep-ph]]

[19] Magg M, Wetterich C. Neutrino mass problem and gauge hierarchy. Physics Letters B. 1980;**94**:61

[20] Lazarides G, Shafi Q, Wetterich C. Proton lifetime and fermion masses in an SO(10) model. Nuclear Physics B. 1981;**181**:287

[21] Mohapatra RN, Senjanovic G. Neutrino masses and mixings in gauge models with spontaneous parity violation. Physical Review D. 1981;**23**:165

[22] Ma E, Sarkar U. Neutrino masses and leptogenesis with heavy Higgs triplets. Physical Review Letters. 1998; **80**:5716. [hep-ph/9802445]

[23] Konetschny W, Kummer W. Nonconservation of total lepton number with scalar bosons. Physics Letters B. 1977;**70**:433

[24] Schechter J, Valle JWF. Neutrino masses in SU(2) × U(1) theories. Physical Review D. 1980;**22**:2227

[25] Cheng TP, Li L-F. Neutrino masses, mixings and oscillations in SU(2) × U(1) models of electroweak interactions. Physical Review D. 1980; **22**:2860

[26] Bilenky SM, Hosek J, Petcov ST. On oscillations of neutrinos with dirac and majorana masses. Physics Letters B. 1980;**94**:495

[27] Zee A. Quantum numbers of majorana neutrino masses. Nuclear Physics B. 1986;**264**:99

[28] Babu KS. Model of 'Calculable' majorana neutrino masses. Physics Letters B. 1988;**203**:132

[29] Chen CH, Nomura T. Bounds on LFV Higgs decays in a vector-like lepton model and searching for doubly charged leptons at the LHC. European Physical Journal C: Particles and Fields. 2016;**76**(6):353. DOI: 10.1140/epjc/s10052-016-4197-3. [arXiv:1602.07519 [hep-ph]]

[30] Chen CH, Nomura T. Single production of $X_{\pm 5/3}$ and $Y_{\mp 4/3}$ vector like quarks at the LHC. Physical Review D. 2016;**94**(3):035001. DOI: 10.1103/PhysRevD.94.035001. [arXiv: 1603.05837 [hep-ph]]

[31] Chen CH, Nomura T, Okada H. Explanation of $B \to K^{(*)}\ell^+\ell^-$ and muon $g-2$, and implications at the LHC. Physical Review D. 2016;**94**(11):115005.

DOI: 10.1103/PhysRevD.94.115005. [arXiv:1607.04857 [hep-ph]]

[32] Chen CH, Nomura T, Okada H. Excesses of muon $g - 2$, $R_{D^{(*)}}$, and $R_K$ in a leptoquark model. Physics Letters B. 2017;**774**:456. DOI: 10.1016/j. physletb.2017.10.005. [arXiv:1703.03251 [hep-ph]]

[33] Aad G et al. [ATLAS Collaboration]. Measurements of the Higgs boson production and decay rates and coupling strengths using pp collision data at $\sqrt{s} = 7$ and 8 TeV in the ATLAS experiment. European Physical Journal C: Particles and Fields. 2016;**76**(1):6. DOI: 10.1140/epjc/s10052-015-3769-y. [arXiv:1507.04548 [hep-ex]]

[34] CMS Collaboration [CMS Collaboration]. Precise determination of the mass of the Higgs boson and studies of the compatibility of its couplings with the standard model. CMS-PAS-HIG-14-009

[35] Amhis Y et al. [HFLAV Collaboration]. Averages of $b$-hadron, $c$-hadron, and $\tau$-lepton properties as of summer 2016. European Physical Journal C. 2017;**77**(12):895. DOI: 10.1140/epjc/s10052-017-5058-4 [arXiv: 1612.07233 [hep-ex]]

[36] Bailey JA et al. [MILC Collaboration]. '$B \rightarrow D\tau\nu$ form factors at nonzero recoil and $|V_{cb}|$ from 2+1-flavor lattice QCD. Physical Review D. 2015;**92**(3):034506. DOI: 10.1103/PhysRevD.92.034506. [arXiv: 1503.07237 [hep-lat]]

[37] Na H et al. [HPQCD Collaboration]. $B \rightarrow Dl\nu$ form factors at nonzero recoil and extraction of $|V_{cb}|$. Physical Review D. 2015;**92**(5):054510. DOI: 10.1103/PhysRevD.93.119906; Erratum: Physical Review D. 2016;**93**(11):119906. DOI: 10.1103/PhysRevD.92.054510 [arXiv: 1505.03925 [hep-lat]]

[38] Aaij R et al. [LHCb Collaboration]. Test of lepton universality using $B^+ \rightarrow K^+\ell^+\ell^-$ decays. Physical Review Letters. 113, 151601 (2014) DOI: 10.1103/PhysRevLett.113.151601. [arXiv:1406.6482 [hep-ex]]

[39] Aaij R et al. [LHCb Collaboration]. Test of lepton universality with $B^0 \rightarrow K^{*0}\ell^+\ell^-$ decays. JHEP. 2017;**1708**:055. DOI: 10.1007/JHEP08(2017) 055 [arXiv:1705.05802 [hep-ex]]

[40] Dowdall RJ et al. [HPQCD Collaboration]. B-Meson decay constants from improved lattice nonrelativistic QCD with physical u, d, s, and c quarks. Physical Review Letters. 2013;**110**(22):222003. DOI: 10.1103/PhysRevLett.110.222003. [arXiv: 1302.2644 [hep-lat]]

[41] Buchalla G, Buras AJ, Lautenbacher ME. Weak decays beyond leading logarithms. Reviews of Modern Physics. 1996;**68**:1125. DOI: 10.1103/RevModPhys.68.1125. [hep-ph/9512380]

[42] Aaij R et al. [LHCb Collaboration]. Measurement of the $B_s^0 \rightarrow \mu^+\mu^-$ branching fraction and effective lifetime and search for $B^0 \rightarrow \mu^+\mu^-$ decays. Physical Review Letters. 2017;**118**(19): 191801. DOI: 10.1103/PhysRevLett.118.191801. [arXiv: 1703.05747 [hep-ex]]

[43] Bobeth C, Gorbahn M, Hermann T, Misiak M, Stamou E, Steinhauser M. $B_{s,d} \rightarrow l^+l^-$ in the standard model with reduced theoretical uncertainty. Physical Review Letters. 2014;**112**: 101801. DOI:10.1103/PhysRevLett.112.101801 [arXiv: 1311.0903 [hep-ph]]

[44] Hiller G, Schmaltz M. $R_K$ and future $b \rightarrow s\ell\ell$ physics beyond the standard model opportunities. Physical Review D. 2014;**90**:054014. DOI: 10.1103/

PhysRevD.90.054014. [arXiv:1408.1627 [hep-ph]]

[45] Alonso R, Grinstein B, Martin Camalich J. Lifetime of $B_c^-$ Constrains explanations for anomalies in $B \to D^{(*)}\tau\nu$. Physical Review Letters. 2017;**118**(8):081802. DOI: 10.1103/PhysRevLett.118.081802. [arXiv:1611.06676 [hep-ph]]

[46] Colquhoun B et al. [HPQCD Collaboration]. B-meson decay constants: A more complete picture from full lattice QCD. Physical Review D. 2015;**91**(11):114509. DOI: 10.1103/PhysRevD.91.114509. [arXiv:1503.05762 [hep-lat]]

[47] Melikhov D, Stech B. Weak form-factors for heavy meson decays: An Update. Physical Review D. 2000;**62**: 014006. DOI: 10.1103/PhysRevD.62.014006. [hep-ph/0001113]

[48] Wang YM, Wei YB, Shen YL, Lü CD. Perturbative corrections to B → D form factors in QCD. JHEP. 2017;**1706**: 062. DOI: 10.1007/JHEP06(2017)062. [arXiv:1701.06810 [hep-ph]]

[49] Sakaki Y, Tanaka M, Tayduganov A, Watanabe R. Testing leptoquark models in $\overline{B} \to D^{(*)}\tau\overline{\nu}$. Physical Review D. 2013;**88**(9):094012. DOI: 10.1103/PhysRevD.88.094012. [arXiv:1309.0301 [hep-ph]]

[50] Chen CH, Geng CQ. Probing new physics in B —> K(*) l+ l− decays. Physical Review D. 2002;**66**:094018. DOI: 10.1103/PhysRevD.66.094018. [hep-ph/0209352]

[51] Belyaev A, Christensen ND, Pukhov A. CalcHEP 3.4 for collider physics within and beyond the Standard Model. Computer Physics Communications. 2013;**184**:1729. [arXiv:1207.6082 [hep-ph]]

[52] Belyaev A, Leroy C, Mehdiyev R, Pukhov A. Leptoquark single and pair production at LHC with CalcHEP/CompHEP in the complete model. JHEP. 2005;**0509**:005. DOI: 10.1088/1126-6708/2005/09/005. [hep-ph/0502067]

[53] Nadolsky PM, Lai HL, Cao QH, Huston J, Pumplin J, Stump D, et al. Implications of CTEQ global analysis for collider observables. Physical Review D. 2008;**78**:013004. [arXiv:0802.0007 [hep-ph]]

[54] Khachatryan V et al. [CMS Collaboration]. Search for single production of scalar leptoquarks in proton-proton collisions at $\sqrt{s} = 8\ TeV$. Physical Review D. 2016;**93**(3):032005. DOI: 10.1103/PhysRevD.93.032005; Erratum: Physical Review D. 2017;**95**(3):039906. DOI: 10.1103/PhysRevD.95.039906. [arXiv:1509.03750 [hep-ex]]